Eur. J. Med. Chem. 36 (2001) 461–467

PII: S0223-5234(01)01232-6/SCO

Short Communication

Synthesis, molecular modelling, and antiproliferative and cytotoxic effects of carbocyclic derivatives of distamycin with chlorambucil moiety

Danuta Bartulewicz[a,*], Krzysztof Bielawski[b], Anna Bielawska[b], Andrzej Różański[a]

[a]Department of Organic Chemistry, Medical Academy of Białystok, Mickiewicza 2c, 15-230 Białystok, Poland
[b]Department of Medicinal Chemistry and Drug Technology, Medical Academy of Białystok, Mickiewicza 2c, 15-230 Białystok, Poland

Received 20 November 2000; revised 28 January 2001; accepted 8 March 2001

Abstract – New carbocylic analogues of distamycin and netropsin with chlorambucil moieties **5**–**8** have been synthesised. Data from the ethidium displacement assay showed that these compounds bind in the minor groove of DNA. The observed reduced affinity to AT pairs and increased affinity towards GC sequences of the carbocyclic lexitropsins with chlorambucil moiety **5**–**8** in comparison with netropsin and distamycin was observed and rationalised by means of molecular modelling techniques. All of the compounds **5**–**8** showed antiproliferative and cytotoxic effects in the standard cell line of the mammalian tumour MCF-7. © 2001 Éditions scientifiques et médicales Elsevier SAS

netropsin / distamycin / carbocyclic analogues of distamycin

1. Introduction

In the course of our investigations of minor-groove-binding drugs, new carbocyclic analogues of netropsin and distamycin **1**–**4** were synthesised and tested for DNA-binding properties (*figure 1*). We have previously shown [1] that these compounds are reversible minor-groove binders with selectivity for AT regions. The replacement of heterocyclic rings by carbocyclic rings [2] yields minor-groove binders which, in comparison with distamycin, have reduced affinity to AT pairs and increased affinity to GC pairs [3], and exhibit lower toxicity and increased antibacterial and antiviral activity [4]. It is worth noting that the carbocyclic analogues of netropsin and distamycin are readily available, can be modified easily and are stable under most experimental conditions [4–6]. Although alkylating agents have a long history in the treatment of cancer, recent interest has focused on the aspects of their sequence-selective action and its possible relationship to cytotoxic potency.

In the present paper, in which we continue our studies of DNA ligands as potential anticancer drugs, we reported a synthesis and a DNA-binding ability of new carbocyclic analogues of distamycin and netropsin with chlorambucil moieties **5**–**8** (*figure 2*). The new compounds have been tested in the standard cell line of the mammalian tumour MCF-7. The DNA-binding ability of these compounds was investigated by an ethidium displacement assay. In addition, in order to rationalise the experimental findings, computer molecular modelling studies were performed with an appropriate B-DNA on the basis of molecular mechanics and molecular dynamics (MD) calculations.

2. Chemistry

The new carbocyclic lexitropsins with chlorambucil moieties were synthesised as outlined in *figure 2*. The preparation of the starting compounds **1**–**4** along with complete spectral characterisation has been re-

* Correspondence and reprints
E-mail address: dbartule@amb.ac.bialystok.pl (D. Bartulewicz).

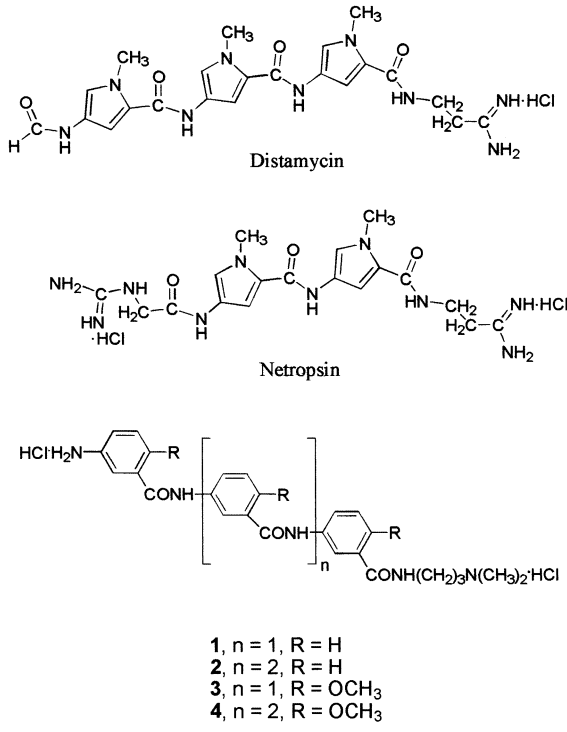

Fig. 1. Structure of distamycin, netropsin and the aminoamides **1**–**4**.

ported in the previous papers [1, 4]. The mustard function was introduced by treatment of the acyl chloride of chlorambucil with the amines **1**–**4** in the presence of DMAP in pyridine. The acid chloride of chlorambucil was prepared by reacting chlorambucil with oxalyl chloride in dry THF.

3. Pharmacology

3.1. Ethidium displacement assay

The apparent DNA-binding constants (K_{app}) of compounds **5**–**8** to calf thymus DNA, poly(dA–dT)·poly(dA–dT), T4 DNA and poly(dG–dC)·poly(dG–dC) were determined using the ethidium displacement assay [7, 8] and compared to those of distamycin and netropsin (*table I*). These data demonstrate that all compounds can bind to the DNAs studied. The apparent binding constants for T4 coliphage DNA for the carbocyclic lexitropsins with chlorambucil moiety gave evidence of their minor-groove selectivity because the major groove of T4 coliphage DNA is blocked by α-glycosylation of the 5-(hydroxymethyl)cytidine residues. Compounds **5**–**8** bind to AT sequences more

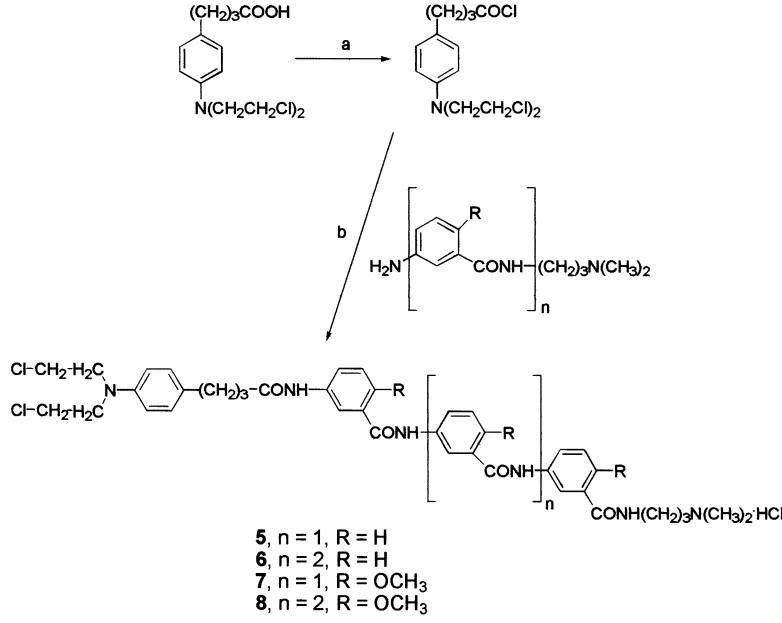

Fig. 2. Synthesis of compounds **5**–**8**: (a) THF, oxalyl chloride, r.t., 2 h; and (b) pyridine, DMAP, 20 h.

Table I. Association constants ($K_{app} \times 10^5$ M^{-1}) of ligands with polynucleotides.

Ligand [a]	Calf thymus DNA	T4 DNA	Poly(dA–dT)$_2$	Poly(dG–dC)$_2$
Ethidium bromide	100 [b]	100 [c]	95 [c]	99 [c]
Netropsin	8.7	8.3	875	2.5
Distamycin	7.5	6.4	340	2.0
5	2.2	2.6	4.2	1.8
6	1.7	1.6	3.4	1.4
7	1.2	1.3	1.9	0.9
8	1.0	1.1	1.8	0.7

[a] The error for netropsin, distamycin and compounds **5**–**8** is $\pm 0.2 \times 10^5$ M^{-1}.
[b] Value from Ref. [6].
[c] Values from Ref. [8].

weakly than the extensively studied minor-groove binders such as netropsin and distamycin. However, these compounds show sequence selectivities. The values of K_{app} of poly(dA–dT)·poly(dA–dT) for **5**–**8** are slightly greater than those for poly(dG–dC)·poly(dG–dC). The K_{app} values of the methoxy derivatives **7** and **8** are comparable to the parent compounds. The results can be explained if it is assumed that all the compounds interact with DNA in the minor-groove-binding mode. The methoxy group is too bulky to insert through the DNA helical stack without disruption of basepairing.

3.2. Cytotoxic and antiproliferative activity of carbocyclic lexitropsins

The described compounds were tested for their antitumour activity in the standard cell line of the mammalian tumour MCF-7. There was an accounted percentage of nonviable cells for every concentration of the drug (*table II*). The IC_{50} data are presented in *table II*. The compounds concentration, which inhibits 50% of colony formation, is in the range 85.7–104.1 μM.

4. Molecular modelling

Computational methods can be useful in modelling ligand–DNA associations to predict the structure and probe the stereochemistry of recognition. After the molecular mechanics refinement calculations, energetically favoured complexes of compounds **5** and **7** with d(CGCGAATTCGCG)$_2$ were obtained (*figure 3*).

Compounds **5** and **7** form centrosymmetric 4 bp complexes with the ligands displaced towards the 5′ end of the 5′-AATT binding site (*figure 3*). This displacement facilitates increased Waals contacts with the walls of the minor groove. In addition to the decreasing affinity for the 5′-AATT-3′ match site, there are weaker contacts with the O2 atom of C21, indicating that the binding-site size requirement for **5** and **7** extends over slightly more than the four central AT base pairs. The energy wells for these ligands within this AT tract are narrow and the data indicate that specific interactions with flanking sequences strongly inhibit ligand translation along the minor groove. The benzene rings of **5** and **7** are positioned roughly in the plane of the bases and the amide groups are located between base pairs. No regular pattern of bifurcated hydrogen bonds then exists. From the analysis of these complexes it appears that van der Waals and electrostatic interactions are more important in stabilising the complexes than specific hydrogen bonds formation. This is consistent with the observed reduced affinity to AT pairs and increased affinity towards GC sequences of the carbocyclic lexitropsins with chlorambucil moieties in comparison with distamycin and netropsin. The protonated terminal dimethylamine nitrogen of the (dimethylamino)propyl tail is adjacent to a negatively charged phosphodiester linkage. The hydrophobic methoxy

Table II. Antitumour activity of compounds **5**–**8** [a].

Compound	Concentration (μg cm^{-3})				IC_{50} [b] (μM)
	0.1	1	10	100	
5	12%	10%	26%	100%	85.69
6	30%	40%	58%	100%	104.12
7	10%	20%	44%	100%	96.89
8	20%	25%	70%	100%	98.62

[a] Indicated as the percentage of nonviable MCF-7 mammal tumour cells.
[b] The compound concentration, which inhibits 50% of colony formation.

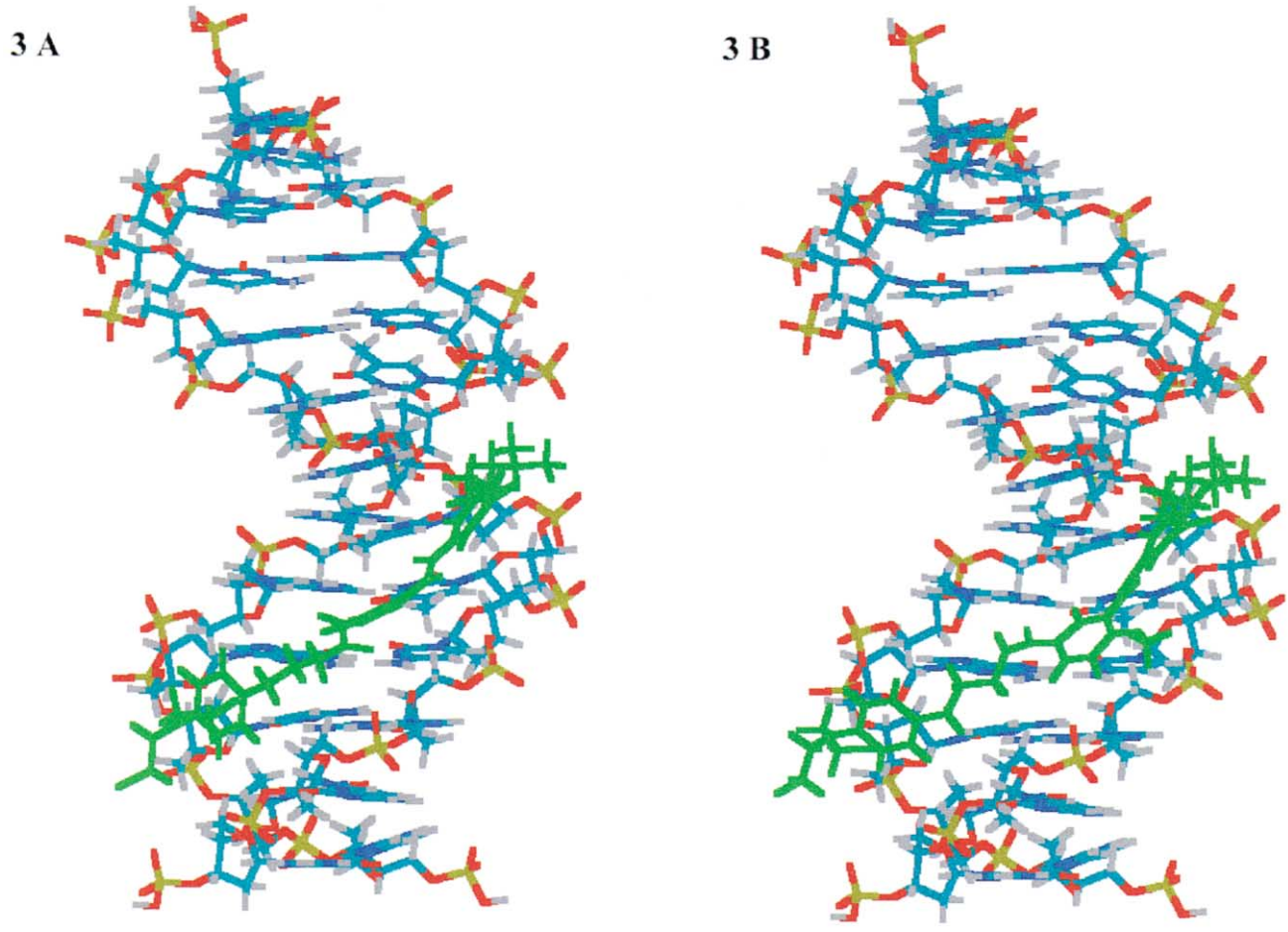

Fig. 3. Views of the low-energy complexes formed between the d(CGCGAATTCGCG)$_2$ and the carbocyclic analogues of distamycin after MD refinement. A, **5**; B, **7**. Ligand molecules are shown in green.

groups of **7** are situated outside the minor groove; therefore, the binding energies for **5** and for **7** are almost the same. Compounds **5** and **7** produce an increase in groove width of ca. 1.5 Å compared with the netropsin–DNA complex [9]. Because of the flexibility of the aliphatic tether of chlorambucil moiety, there is probably a limited distribution of alkylation sites derived from an individual binding complex rather than a unique alkylation site for each individual bound compound. An accurate definition by molecular modelling of the optimal binding site for the compounds studied alone has been hampered by the fact that the DNA fragment used in the model contains a limited number of binding sites.

5. Conclusions

The in vitro experimental findings revealed that all the carbocyclic lexitropsins with chlorambucil moiety **5**–**8** exhibit sufficient tumour cell cytotoxicity towards the standard cell line of the mammalian tumour MCF-7. Moreover, the DNA-binding studies reflect a binding affinity for these compounds that is weaker than for netropsin and distamycin, but analytically reliable. The enhanced flexibility of compounds **5**–**8** would lower the probability of their occupying the correct region of conformational space and increase the entropy loss upon binding, both of which will lead to decreasing binding affinities. It may explain the lower DNA-binding properties of compounds **5**–**8** when compared with

netropsin and distamycin. Molecular modelling calculations made it possible to understand the reason for the observed reduced affinity to AT pairs and increased affinity towards GC sequences of the carbocyclic lexitropsins with chlorambucil moiety in comparison with netropsin and distamycin. Further investigations on the mechanisms of the cytotoxicity carried out by these compounds are in progress.

6. Experimental protocols

6.1. Chemistry

Melting points were determined on a Buchi 535 apparatus and are uncorrected. ^{1}H NMR and ^{13}C NMR spectra were recorded on a Bruker AC 200 F spectrometer using tetramethylsilane as an internal standard. Chemical shifts are expressed in δ value (ppm). Multiplicity of resonance peaks is indicated as singlet (s), doublet (d), triplet (t), quartet (q), broad singlet (bs) and multiplet (m).

Thin-layer chromatograms were prepared on precoated plates (Merck, silica gel 60F-254) using the solvent system (all proportions by volume) methanol–25% ammonia, 99:1. Silica gel 60 (230–400 mesh ASTM) was used for column chromatography.

6.1.1. General procedure

4-[*p*-[Bis(2-chloroethylamino)phenyl]butyric chloride was prepared by dissolving chlorambucil (140 mg, 0.46 mmol) in anhydrous tetrahydrofuran (20 mL) and oxalyl chloride (3 mL), and warming to mild reflux under a drying tube for 2 h. The excess oxalyl chloride and solvent were removed under reduced pressure and the residue co-evaporated with a dry dichloromethane (5 mL, twice). The above acid chloride dissolved in a dry dichloromethane (20 mL) was added dropwise to a chilled (0°C) solution of the aminoamide **1**–**4** (0.42 mmol) in dry pyridine (20 mL) with 4-(dimethylamino)pyridine (DMAP) under stirring. The reaction mixture was kept at 0°C for an additional 15 min, then stirred at room temperature (20 h). The reaction mixture was concentrated under a reduced pressure to a brown foam. The crude product was purified by column chromatography (silica gel) with a methanol gradient (1%, then 1% increase every 100 mL) in chloroform as eluent. After removal of the solvent, the pure chlorambucil derivatives **5**–**8** were obtained as glaze solids.

6.1.1.1. *N-[3-(3-[4-Bis(2-chloroethyl)aminophenylbutyramido]benzamido)-benzoyl]-N′,N′-dimethyl-1,3-propanediamine hydrochloride* ***(5)***

Yield: 0.14 g (45.8%). ^{1}H NMR (DMSO-d_6, δ ppm): 1.20 (m, 2H, CH_2); 1.83 (m, 4H, CH_2); 2.40 (t, 2H, CH_2); 2.72 (s, 6H, $N(CH_3)_2$); 3.09 (m, 2H, CH_2); 3.35 (m, 2H, CH_2); 3.88 (s, 8H, $ClCH_2CH_2N$); 6.63–8.78 (m, 10H, Ar-H); 10.36, 10.49 2× (s, 1H, CONH); 10.83 (bs, 1H, CONH). ^{13}C NMR (DMSO-d_6, δ ppm): 24.15 (CH_2); 27.12 (CH_2); 33.61 (CH_2); 35.83 (CH_2); 36.45 ($CONHCH_2$); 41.87 ($N(CH_3)_2$); 39.80, 52.23 ($ClCH_2CH_2N$); 54.40 ($CH_2N(CH_3)_2$); 111.91; 118.66; 119.89; 121.96; 122.18; 123.15; 127.32; 128.46; 128.63; 129.31; 129.84; 134.89; 135.33; 139.25; 139.58; 141.70; 144.40; 146.17 (Ar); 165.74; 166.36; 171.46 (3×CONH). Anal. Found: C, 59.97; H, 6.56; Cl, 16.24; N, 10.65. Calc. for $C_{33}H_{41}N_5O_3Cl_2HCl$: C, 59.77; H, 6.38; Cl, 16.04; N, 10.56%.

6.1.1.2. *N-[3-(3-(3-[4-Bis(2-chloroethyl)aminophenylbutyramido]benzamido)benzamido)benzoyl]-N′,N′-dimethyl-1,3-propanediamine hydrochloride* ***(6)***

Yield: 0.17 g (46.2%). ^{1}H NMR (DMSO-d_6, δ ppm): 1.84–1.94 (m, 4H, CH_2); 2.37 (t, 2H, CH_2); 2.43 (s, 6H, $N(CH_3)_2$); 2.64 (m, 4H, CH_2); 3.44 (t, 2H, CH_2); 3.65 (m, 8H, $ClCH_2CH_2N$); 6.58–8.16 (m, 10H, Ar-H). ^{13}C NMR (DMSO-d_6, δ ppm): 25.99 (CH_2); 27.41 (CH_2); 33.61 (CH_2); 34.40 (CH_2); 36.40 ($CONHCH_2$); 40.54 ($N(CH_3)_2$); 39.18; 53.53 ($ClCH_2CH_2NH_2$); 56.72 ($CH_2N(CH_3)_2$); 112.23; 112.27; 119.11; 119.60; 120.06; 123.21; 123.36; 123.68; 123.81; 124.12; 124.53; 129.13; 129.21; 129.48; 129.64; 130.56; 134.87; 135.21; 135.46; 138.61; 138.70; 144.51 (Ar); 167.30; 167.39; 168.70; 173.31 (4×CONH). Anal. Found: C, 61.31; H, 6.06; Cl, 12.58; N, 10.07. Calc. for $C_{41}H_{47}N_6O_4Cl_2HCl$: C, 61.92; H, 6.08; Cl, 13.38; N, 10.57%.

6.1.1.3. *5-{5-[4-[Bis(2-chloroethyl)aminophenyl]butyramido]-2-methoxybenzamido}-N-[3-(dimethylamino)propylo]-2-methoxybenzeno-1-carboxamide hydrochloride* ***(7)***

Yield: 0.14 g (42.7%). ^{1}H NMR ($CDCl_3/CD_3OD$, δ ppm): 1.87 (m, 2H, CH_2); 2.08 (m, 2H, CH_2); 2.26 (t, 2H, CH_2); 2.48 (t, 2H, CH_2); 2.75 (s, 6H, $N(CH_3)_2$); 3.18 (t, 2H, CH_2); 3.54 (t, 2H, CH_2); 3.84 (s, 8H, $ClCH_2CH_2N$); 3.92 2× (s, 3H, OCH_3); 6.65–8.00 (m, 10H, Ar-H). ^{13}C NMR ($CDCl_3/CD_3OD$, δ ppm): 24.57 (CH_2); 27.10 (CH_2); 33.86 (CH_2); 36.13 (CH_2); 36.22 ($CONHCH_2$); 42.56 ($N(CH_3)_2$); 40.29; 53.29 ($ClCH_2CH_2N$); 55.22 ($CH_2N(CH_3)_2$); 56.01; 56.24 (2×

OCH_3); 106.69; 111.82; 111.96; 122.63; 123.65; 125.42; 125.73; 129.39; 130.62; 130.48; 131.13; 132.33; 138.62; 144.07; 153.38; 154.29 (Ar) 163.41; 166.12; 172.35 (3×CONH). Anal. Found: C, 58.01; H, 6.70; Cl, 14.29; N, 9.26. Calc. for $C_{35}H_{45}N_5O_5Cl_2HCl$: C, 58.13; H, 6.41; Cl, 14.71; N, 9.68%.

*6.1.1.4. 5-{5-[4-[Bis(2-chloroethyl)aminophenyl]-butyramido]-2-methoxybenzamido}-N-[3-(dimethyl-amino)propyl]-2-methoxybenzene-1-carboxamide hydrochloride (**8**)*

Yield: 0.21 g (51.9%). ^{1}H NMR ($CDCl_3$, δ ppm): 1.78 (m, 4H, CH_2); 2.25 (s, 6H, $N(CH_3)_2$); 2.37 (m, 4H, CH_2); 3.54 (m, 4H, CH_2); 3.93 (s, 3H OCH_3); 3.98 (s, 6H, OCH_3); 4.11 (m, 8H, $ClCH_2CH_2N$); 7.02–8.18 (m, 13H, Ar-H); 8.25 (t, 1H, CONH); 8.60; 8.82; 9.79 3× (s, 1H, CONH). ^{13}C NMR ($CDCl_3$, δ ppm): 22.66 (CH_2); 27.29 (CH_2); 29.33 (CH_2); 31.88 (CH_2); 38.41 (CH_2); 45.56 ($N(CH_3)_2$); 40.95; 53.10 ($ClCH_2CH_2N$); 55.02 ($CH_2N(CH_3)_2$); 56.19; 56.43; 56.68 (3×OCH_3); 112.02; 113.38; 117.05; 119.74; 120.42; 121.72; 122.04; 122.26; 122.81; 123.61; 125.11; 127.88; 129.05; 129.88; 130.90; 132.46; 137.62; 143.98; 146.97; 151.96; 152.50; 153.85; 156.78; 159.11 (Ar); 162.21; 162.78; 163.15; 164.83 (4× CONH). Anal. Found: C, 59.45; H, 5.97; Cl, 11.89; N, 9.13. Calc. for $C_{44}H_{53}N_5O_7Cl_2HCl$: C, 59.69; H, 6.15; Cl, 12.01; N, 9.49%.

6.2. Pharmacology

6.2.1. Ethidium displacement assay

Ethidium bromide, netropsin, distamycin, calf thymus DNA, poly(dA–dT)·poly(dA–dT), T4 DNA and poly(dG–dC)·poly(dG–dC) were purchased from Sigma Chemical Co. Fluorescence was measured on a Hitachi spectrophotometer F-2500 FL at room temperature. The DNA–ethidium complex was excited at 546 nm and the fluorescence was measured at 595 nm. To 2 mL of ethidium bromide buffer, pH 7.4, was added 25 μL of DNA solution ($A_{260} = 2$) and the maximum fluorescence was measured. Aliquots of a 10 mM stock drug solution (1 mg of drug to be tested and the appropriate volume of distilled water to make a 10 mM solution) were then added to the DNA–ethidium solution and the fluorescence was measured after each addition until a 50% reduction of fluorescence had occurred. If the 10 mM stock solution lowered the percent fluorescence too quickly, the solution was further diluted to 1 mM prior to titration. The fluorescence intensity data points were fit to theoretical curves with one or two different iterative nonlinear least-squares computer routines. The apparent binding constant was calculated from:

$$K_{EtBr}[EtBr] = K_{app}[drug]$$

where [drug] is the concentration of drug at a 50% reduction of fluorescence and K_{EtBr} is known [6, 7]. The compounds **5–8** and their DNA-bound complexes showed neither optical absorption nor fluorescence at 595 nm and did not interfere with the fluorescence of an unbound ethidium.

6.2.2. Cytotoxic and antiproliferative activity

6.2.2.1. Cells

Human breast cancer cells (MCF-7) were purchased from the American Type Culture Collection (Rockville, MD) and maintained in Dulbecco modified Eagle medium supplemented with 2 mM glutamine, 8% heat-inactivated foetal bovine serum and the investigated compounds **5–8**. The cells were grown in 75 cm^3 flasks in a culture incubator at 37°C in a humid atmosphere containing 5% CO_2. The cells, after inducing apopthosis, were cultured in Costar flasks and subconfluent cells were detached with 0.05% trypsin and 0.02% EDTA in a calcium-free phosphate-buffered saline. The cells reached about 80% confluence at day 3 after which, in most cases, these cells were used for the assays.

Compounds **5–8** were dissolved in sterile water and used at concentrations of 0.1, 1, 10 and 100 μg cm^{-3}.

6.2.2.2. Determination of IC_{50}

MCF-7 grown in 6-well plates were stained during evaluation of the time course of compound action with a dye mixture (10 μM acridine orange and 10 μM ethidium bromide) that was prepared in phosphate-buffered saline. Acridine orange (fluorescent DNA-binding dye) intercalates into DNA, making it appear green, and binds to RNA, staining it red-orange. Ethidium bromide is taken up only by nonviable cells, its fluorescence overwhelming that of the acridine orange and making the chromatin of the lysed cells appear orange. At the appropriate time point 250 μL of the cell suspension was mixed with 10 μL of the dye mix and 200 cells per sample were examined by fluorescence microscopy.

6.3. Molecular modelling

Initial structures for the molecules **5** and **7** were constructed using the HyperChem version 5.11 program, which was also used for manipulation and interactive

docking manoeuvres. The conformational searching in torsional space was performed using the multiconformer method [10]. Energy minima for **5** and **7** were determined by a semi-empirical method AM1 (as implemented in HyperChem 5.11). The conformations thus obtained were confirmed as minima by vibrational analysis. Atom-centred charges for each molecule were computed from the AM1 wavefunctions (HyperChem 5.11) by the procedure of Orozco and Luque [11], which provides derived charges that closely resemble those obtainable from ab initio 6-31G* calculations. The terminal dimethylamine nitrogen of the (dimethylamino)propyl tail ($pK_a \sim 9.3$) of ligands **5** and **7** was assumed to be singly protonated. Initial coordinates for the 12-mer DNA duplex host were taken from the crystal structure of the $d(CGCGAATTCGCG)_2$ complex from the Brookhaven Protein Databank (PDB file 1 bna). Initial models for each complex were constructed by docking the ligands at a core A4-T7 location within the minor groove with: (a) 1:1 stoichiometry; (b) the concave surface of the molecules facing the convex groove floor; and (c) fully extended, all-*trans* ligand conformations. Ligands **5** and **7** are asymmetric in structure; therefore, two alternative orientations of these for compounds in the minor groove of DNA were considered. A rigid-body refinement procedure was used to align the ligand molecules with the walls of the minor groove, and to remove unfavourable atomic contacts, prior to energy minimisation. For compounds **5** and **7** alternative positions of the compounds were considered by translation of the ligand along the 5′-AATT-3′ minor-groove tract of DNA. Ligand displacements were restricted ±2 bp from an initial location. The AMBER force field (as implemented in HyperChem 5.11) was used for all energy calculations [12, 13]. van der Waals and H-bonded energy terms were included up to 8 Å but explicit base pair restraints were not used. Solvent and counterions were not included explicitly for reasons of computational expense. Instead, their effect was simulated using a simple distance-dependent dielectric constant with $\varepsilon = 4r_{ij}$. This formalism is well established in the field of protein modelling and has been tested in some detail for a nucleic acid model system with satisfactory results [14]. The DNA–ligand complexes were initially regularised by conjugate-gradient molecular modelling to reduce poor intermolecular steric contacts so as to minimise the energy of the bound ligand alone and for minimisation of the unrestrained complex to an energy gradient of <0.01 kcal $(Å\ mol)^{-1}$. MD simulations of each complex were subsequently performed for 5 ps (integration time step = 1 fs) at 300 K. Potential energy analysis during MD progress showed that the systems reached equilibrium rapidly, typically at (times of) <2 ps. Atomic coordinates were sampled at 0.2 ps intervals during the simulation period. In each case, the averaged structure from the accumulated snapshots was subjected to final molecular mechanics relaxation. The Polak–Ribiere minimization method was applied with a gradient value of 0.01 to test for convergence, to generate the refined complex.

References

[1] Bartulewicz D., Markowska A., Wołczynski S., Dąbrowska M., Różański A., Acta Biochim. Pol. 47 (2000) 23–35.

[2] Dasgupta D., Rajagopalan M., Sasisekharan V., Biochem. Biophys. Res. Commun. 140 (1986) 626–631.

[3] Rao S., Sasisekharan V., Indian J. Chem. 29B (1990) 508–513.

[4] Bartulewicz D., Bielawski K., Markowska A., Zwierz K., Różański A., Acta Biochim. Pol. 45 (1998) 41–57.

[5] Yan Y., Liu M., Gong B., Bioorg. Med. Chem. Lett. 7 (1997) 1469–1474.

[6] Lee M., Rhodes A.L., Wyatt M.D., D'Incalci M., Forrow S., Hartley J.A., J. Med. Chem. 36 (1993) 863–870.

[7] Morgan A.R., Lee J.S., Pulleyblank D.F., Murray N.L., Evans D.H., Nucleic Acids Res. 7 (1979) 547–569.

[8] Debart F., Periguad C., Gosselin D., Mrani D., Rayner B., Le Ber P., Auclair C., Balzarini J., De Clercq E., Paoletti C., Imbach J.L., J. Med. Chem. 32 (1989) 1074–1083.

[9] Kopka M.L., Yoon Ch., Goodsell D., Pjura P., Dickerson R.E., Proc. Natl. Acad. Sci. USA 82 (1985) 1376–1380.

[10] Lipton M., Still W.C., J. Comput. Chem. 9 (1988) 345–355.

[11] Orozco M., Luque F.J., J. Comput. Chem. 11 (1990) 909–923.

[12] Weiner S.J., Kollman P.A., Case D.A., Singh U.C., Ghio G., Alagano G., Profeta S., Weiner P., J. Am. Chem. Soc. 108 (1984) 765–784.

[13] Weiner S.J., Kollman P.A., Nguyen D.T., Case D.A., J. Comput. Chem. 7 (1986) 230–252.

[14] Orozco M., Laughton C.A., Herzyk P., Neidle S., J. Biomol. Struct. Dyn. 8 (1990) 359–373.